ORIGINAL PAPER

DEVELOPMENT OF A MODEL FOR THE CRACK INITIATION AND GROWTH SIMULATION OF THE STRUCTURAL MATERIALS UNDER LIQUID METAL EMBRITTLEMENT CONDITIONS

LIVIA STOICA[1], VASILE RADU[1], ALEXANDRU NITU[1], ILIE PRISECARU[2]

Manuscript received: 10.07.2021; Accepted paper: 01.09.2021;
Published online: 30.09.2021.

Abstract. *The paper develops a model based on the finite element analysis of the crack initiation and propagation in the generation IV structural materials due to the liquid metal embrittlement (LME) phenomenon. The stress-strain experimental curves obtained at 400 ºC by testing in the liquid lead and air were converted as the Ramberg - Osgood constitutive equations by proposing a new method to obtain the strain hardening coefficient. To estimate the accuracy of prediction are used the residual and standardised residual in the context of regression analysis. Further, a model based on the Gurson–Tvergaard-Needleman approach (GTN) was set up to evaluate the crack initiation and propagation under the LME conditions. An application of the developed micro-mechanical model that predicts the crack initiation and propagation in the Compact –Tension (CT) specimen due to LME is performed. The model is practical in the structural integrity activities framework of the structural materials that will be used in the ALFRED demonstrator, which will be build-up at RATEN ICN, Romania.*

Keywords: *liquid metal embrittlement; stress-strain equation; fracture mechanics; finite element analysis.*

1. INTRODUCTION

In the research area for the Generation IV nuclear reactors, a vital task is to manage the structural integrity of the nuclear components under representative environment conditions. Thus, the target to confirm a demanding safety of functioning and operation for the nuclear facilities by considering the aggressive and damaging factors as irradiation, high temperature, and corrosion, constitutes a priority even from the design stage. Nowadays, within the R&D studies dedicated to nuclear systems using corrosive lead or Lead Bismuth Eutectic (LBE) as a coolant, the compatibility is usually related to reduced or controlled corrosiveness.

In the literature [1] the degradation mechanisms of the mechanical properties by liquid metals were mainly classified as liquid metal embrittlement (LME) and liquid metal-assisted damage (LMAD). Common features of those degradation mechanisms involve a physicochemical and mechanical process, and therefore the interpretation of which is essentially supported the wetting concept.

There is a large kind of mechanism that is proposed to explain LME. The subsequent definition for the liquid metal embrittlement is accepted: LME is the loss of tensile ductility

[1] Department of Nuclear Material and Corrosion, RATEN Institute for Nuclear Research, 115400 Mioveni, Romania. E-mail: livia.stoica@nuclear.ro.
[2] University Politehnica of Bucharest, 060042 Bucharest, Romania.

of stressed normally ductile metals or metallic alloys in contact with a liquid metal that may lead to brittle fracture [2-4]. Taking under consideration the resistance of stainless steel to LME, modelling can be instructive to the overall understanding of LME resistance, but also to use it in the practical applications associated with assessing the structural integrity for the systems in Generation IV reactors.

In the present paper, based on the stress-strain constitutive equation (Ramberg-Osgood type) resulted from the experimental curves from the testing of 316L stainless-steel in the air and liquid lead at 400°C, is developed an application under LME conditions. Thus, a model supported on the Gurson - Tvergaard - Needleman approach (GTN) was set up to evaluate by the finite element modelling the crack initiation and propagation promoted by the LME conditions within the fracture mechanics framework methodology.

The first chapter makes a brief overview of the GTN approach to describe crack initiation and propagation in metals. Ramberg - Osgood constitutive equation [5] that describes mechanical behaviour under tensile loading are presented in the next chapter, and a new solution to obtain numerically the strain-hardening coefficient is proposed. To estimate the accuracy of prediction are used the residual and standardised residual in the context of regression analysis. The Slow Strain Rate Tensile (SSRT) experiments are performed with 316L specimens in the air and liquid lead at 400°C and results are exposed. The elaborated model of Compact-Tension is analyzed with specialized fracture mechanics software FEACrack by finite element method, and also the results are discussed.

2. GURSON MODEL PARAMETERS FOR DUCTILE FRACTURE SIMULATION

The ductile fracture process in metals has been modelled by using the uncoupled or the coupled models [6]. The Gurson model [7] and next to its developments [8, 9] fall in the category of micromechanical-based coupled models. In the reference [7], Gurson proposed a yield criterion and the flow rules for the rigid plastic porous material. The Gurson yield criterion was adapted by Tvergaard [9] to consider the void interaction effects. In the reference [8], Tvergaard and Needleman adjusted the Gurson model to account for the quick loss of ability to support a mechanical load of the material at the onset of the micro-void coalescence. This last form of the Gurson model is mentioned as the GTN model. It is often used to model ductile fracture in metals.

Gurson [7] proposed for porous materials a yield potential. This yield potential was obtained using cell studies with a concentric spherical void. Thus, the macroscopic yield potential considers the terms called the void volume fraction (f). The void volume fraction signifies the ratio of the void volume to cell volume. Further, Tvergaard [9] improved the Gurson model to consider the micro-void interaction employing three additional void interaction parameters ($q_1=1.5$, $q_2=1.0$, and $q_3=2.25$). Moreover, the void growth rate is improved after a specific void volume fraction, termed the critical void volume fraction (f_c).

The plastic potential of the GTN model has the next expression:

$$\Phi\left(\sigma_e,\sigma_h,f^*,\sigma_y\right)=\left(\frac{\sigma_e}{\sigma_h}\right)^2+2f^*\cdot q_1\cdot\cosh\left(q_2\cdot\frac{3\sigma_h}{2\sigma_y}\right)-1-q_3\left(f^*\right)^2=0 \quad (1)$$

where:

- σ_e is the effective stress;
- σ_h is the hydrostatic stress;
- $\sigma_y=\sigma_y\left(\varepsilon_p\right)$ represents the strain-hardening curve defined in terms of the effective

plastic strain ε_p;

- f^* is the adjusted void volume fraction.

The accelerated void growth is started when the void volume fraction (f^*) go beyond the critical void volume fraction (f_c). Also, the accelerated void growth factor (*K*) increases the void growth until the failure void volume fraction (f_F) is gotten.

The adjusted void volume fraction in the GTN model is:

$$f^* = \begin{cases} f, & f \le f_c \\ f_c + K \cdot (f - f_c), & f_c < f < f_F \end{cases} \tag{2}$$

where:

$$K = \frac{\bar{f}_F - f_c}{f_F - f_c}, \tag{3}$$

with:

$$\bar{f}_F = q_1 + \frac{\sqrt{q_1^2 - q_3}}{q_3}. \tag{4}$$

The increase in void volume fraction is because of the growth of existing voids and so the nucleation of new voids. The void nucleation rate is proportional to the effective plastic strain rate:

$$\dot{f}_N = C \cdot \dot{\varepsilon}_p \tag{5}$$

To express the proportionally constant *C*, a Gaussian distribution is used:

$$C = \frac{f_N}{s_N \cdot \sqrt{2\pi}} \cdot \exp\left[-\frac{1}{2} \left(\frac{\varepsilon_p - \varepsilon_N}{s_N} \right)^2 \right] \tag{6}$$

Here ε_N is the mean nucleation strain with a standard deviation s_N, and f_N is the volume fraction of nucleating voids. After all, the GTN model has nine parameters, which could be classified into three categories: q_1, q_2, q_3 stand the void interaction parameters; f_0, f_N, ε_N, s_N stand the material parameters; f_c, f_F stand the ductile fracture parameters.

The hardening relationship $\sigma_y = \sigma_y(\varepsilon_p)$ is required so on finish describe the GTN model. Within the current approach, the GTN model will be set up to describe the crack initiation and propagation in the Compact–Tension (CT) specimen, with the characteristics of 316L from the Slow Strain Rate Testing (SSRT) tests in the air and the liquid lead.

3. RAMBERG – OSGOOD CONSTITUTIVE EQUATION

To simulate the crack initiation and propagation in the CT specimen by finite element analyses, there is a need for the description of the strain-hardening behaviour of materials using mathematical expression between mechanical stress and strain of materials.

With the scope to describe the strain-hardening behaviour of materials using the experimental stress versus strain material curves, in the literature are reported various

methods. In the reference [10] is described a computer program that fits the analytical expressions to experimental stress-strain data for the Ramberg-Osgood description. Some quantities resulting from data contain yield strength, plastic strain component, tangent moduli and value of Poisson's ratio. Reverse engineering methodology from reference [11] proposed obtaining the strain hardening exponent and strength coefficient for tensile loading. The reference [12] proposes a generalization of Kamaya's method for the materials with Luder's strains. These approaches use relative complex procedures and each of them requests implementation scripts in programming environments.

ASTM E646-07 [13] describes the test method to obtain the tensile strain-hardening exponents n, and utilizes stress-strain data resulted in a uniaxial tension test. In this method, the strain-hardening exponents are obtained from an empirical representation over the array of interest of the true-stress versus true-strain curve.

In the present paper, a fracture mechanics parameter, *J*-integral will be used in the evaluation of crack tip conditions which determine the extinction of finite elements from the front of the crack to simulate crack initiation and propagation.

Next, we will describe the proposed method of obtaining the Ramberg Osgood equation.

The engineering stress-strain curve is not a true indication of the deformation characteristics of a metal. The curve which is known as a true-stress versus true-strain curve is often also known as a flow curve since it represents the basic plastic-flow characteristics of the material.

The true stress (σ) and true strain (ε) are defined as [14]:

$$\sigma = \frac{P}{A_0}(1+e) \tag{7}$$

$$\varepsilon = \ln(1+e) \tag{8}$$

$$e = \frac{\Delta L}{L_0}, \tag{9}$$

where: P - instantaneous load; A_0 - original cross-sectional area of the specimen; e - engineering strain; ΔL - total specimen deformation; L_0 - initial specimen length.

The mathematical relationship which expresses the true stress-strain curve is a power curve [14, 15]. The Ramberg - Osgood flow rule states that, for quasi-static loading at a given temperature and strain rate, the true stress σ is given as a function of the strength coefficient *K*, strain-hardening exponent *n*, and true plastic strain ε_p as:

$$\sigma = K\varepsilon_p^n \tag{10}$$

where: n - is the strain-hardening coefficient; K - is the strength coefficient.

The instability in tension loading that occurs into a specimen is known as the necking phenomenon. Necking or localized deformation generally begins at maximum load during the tensile deformation of a ductile metal [14]. Let consider the definition of stress:

$$P = \sigma \cdot A, \tag{11}$$

where: P - the mechanical load; σ - the stress; A - cross-sectional area of the specimen.

The condition of instability resulting in localized deformation is defined by condition:

$$dP = \sigma \cdot dA + A \cdot d\sigma = 0 \tag{12}$$

From the constancy of specimen volume:

$$\frac{dL}{L} = -\frac{dA}{A} \tag{13}$$

is obtained

$$-\frac{dA}{A} = \frac{dL}{L} = d\varepsilon_p \tag{14}$$

where ε is the strain.

From (12) with (14) results:

$$\frac{d\sigma}{\sigma} = d\varepsilon_p \text{ or, } \frac{d\sigma}{d\varepsilon_p} = \sigma \tag{15}$$

From equation (10) it is obtained:

$$\frac{d\sigma}{d\varepsilon_p} = nK\varepsilon_p^{n-1} \tag{16}$$

By combining (15) with (16):

$$\sigma = nK\varepsilon^{n-1}$$

To determine the strain at which the necking occurs it used the equation:

$$\sigma = K\varepsilon_p^n = nK\varepsilon_p^{n-1} \tag{17}$$

This means that the strain at which necking occurs ε_u is numerically equal to the strain hardening coefficient [14]:

$$\varepsilon_u = n \tag{18}$$

Based on this assertion, the present paper proposes a new method to obtain the strain hardening coefficient, from the stress-strain curve. The relationship (10), which describes the flow curve, could be written for yield point pair (σ_y, ε_y) and the necking pair (σ_u, ε_u):

$$\sigma_y = K \cdot \varepsilon_y^n \tag{19}$$

Respectively,

$$\sigma_u = K \cdot \varepsilon_u^n \tag{20}$$

From relationship (19) and (20) is obtained:

$$\frac{\sigma_u}{\sigma_y} = \left(\frac{\varepsilon_u}{\varepsilon_y}\right)^n \tag{21}$$

and, by logarithm:

$$\ln\left(\frac{\sigma_u}{\sigma_y}\right)=n\left[\ln\left(\varepsilon_u\right)-\ln\left(\varepsilon_y\right)\right] \tag{22}$$

Considering relationship (18) results in a transcendental equation for strain hardening coefficient:

$$\ln\left(\frac{\sigma_u}{\sigma_y}\right)=n\left[\ln\left(n\right)-\ln\left(\varepsilon_y\right)\right] \tag{23}$$

Equation (23) is numerically solved in the mathematical computing software Matlab [16] for the present paper. The Ramberg - Osgood equation (10) could even be put in another form, which is mostly utilized within the finite element software. Starting from equation (10), results:

$$\varepsilon_p=\left(\frac{\sigma}{K}\right)^{\frac{1}{n}} \tag{24}$$

and this becomes

$$\varepsilon-\varepsilon_e=\left(\frac{\sigma}{K}\right)^{\frac{1}{n}} \tag{25}$$

where: ε - the total strain; ε_e - the elastic strain. But the elastic strain is

$$\varepsilon_e=\frac{\sigma}{E} \tag{26}$$

and E is the Young modulus of elasticity. With (26) in (25),

$$\varepsilon=\frac{\sigma}{E}+\left(\frac{\sigma}{K}\right)^{\frac{1}{n}} \tag{27}$$

By introducing the next new parameters

$$\left(\frac{1}{K}\right)^{\frac{1}{n}}=\alpha\cdot\frac{\sigma_0^{1-\frac{1}{n}}}{E} \tag{28}$$

the Ramberg - Osgood equation becomes

$$\varepsilon=\frac{\sigma}{E}+\alpha\cdot\frac{\sigma_0}{E}\cdot\left(\frac{\sigma}{\sigma_0}\right)^{\frac{1}{n}} \tag{29}$$

with: α - material parameter; n - strain-hardening coefficient; σ_0 - reference stress. Finally, the last format of Ramberg - Osgood equation is

$$\frac{\varepsilon}{\frac{\sigma_0}{E}}=\frac{\sigma}{\sigma_0}+\alpha\cdot\left(\frac{\sigma}{\sigma_0}\right)^{\frac{1}{n}} \text{ or } \frac{\varepsilon}{\varepsilon_0}=\frac{\sigma}{\sigma_0}+\alpha\cdot\left(\frac{\sigma}{\sigma_0}\right)^{\frac{1}{n}} \tag{30}$$

Equation Ramberg - Osgood (30) is completely determined if α and *n* are known. By solving equation (23), is obtained the strain-hardening coefficient *n*. To obtain α, in equation (29) we take $\sigma = \sigma_0 = \sigma_y$ and results

$$\varepsilon - \frac{\sigma_y}{E} = \alpha \cdot \frac{\sigma_y}{E} \tag{31}$$

As σ_y is the yield stress with the plastic deformation of 0.2%, results:

$$\alpha = \frac{0.002 \cdot E}{\sigma_y} \tag{32}$$

From the experimental stress-strain curve it was determined α and *n* parameters, and the equation Ramberg - Osgood as well in the format from (30), and further it will be employed within the finite element analyses software.

A comparison between the proposed solution from the present paper and the approach described in the ASTM E646-07 [13] is made in the next chapter concerning the strain-hardening coefficient *n*.

The fracture mechanics analyses use the *J*-integral fracture mechanics parameters at the crack-tip [15]. *J*-integral completely describes the conditions within the crack tip plastic zone. The fracture mechanics software called FEACrack [17] used in the present paper includes built-in *J*-integral post-processing algorithms.

4. THE EXPERIMENTAL TESTS IN THE LIQUID LEAD AND AIR ENVIRONMENTS

The experimental tests on the 316L stainless steel specimens, used in Generation IV reactors as the structural material, were performed in both liquid lead and the air environment to highlight better the material behaviour under the liquid metal embrittlement. The specimens were tested in the air and liquid lead at the strain rate of 10^{-5} s^{-1} and the temperature of 400°C according to ASTM - G129-00 [18] and ASTM E8/8M [19].

After the SSRT tests in the air and liquid lead, it is used the methodology proposed in chapter 3 to obtain the strain-hardening coefficient *n* and the material parameter α from the stress-strain curves. Thereby, the constitutive equations, in the Ramberg - Osgood format are obtained.

To see the difference between the experimental curves in the air and the liquid lead and those predicted by Ramberg - Osgood solutions are used the residual and standardised residual statistical parameters [20].

The residual is defined as:

$$Residual = \sigma_{exp} - \sigma_{pred} \tag{33}$$

Also, the standardized residual is the ratio between the individual raw residual and the standard deviation. Residual standard deviation is:

$$S_{res} = \sqrt{\frac{\Sigma(\sigma_{exp} - \sigma_{pred})^2}{n-2}} \tag{34}$$

where:

S_{res} - Residual standard deviation;

σ_{exp} - Experimental value of stress;

σ_{pred} - Predicted (estimated) value of stress;

n - data point in population.

However, the standardized residual offers a reliable measure of the error of the prediction:

$$Standardised\ residual = \frac{Residual}{S_{res}} \tag{35}$$

The literature [20] notes that standardised residuals must be $S_{res} < 3$, to have a good prediction. In the air, the Ramberg - Osgood constitutive equation for 316L at 400°C is:

$$\frac{\varepsilon}{\varepsilon_0} = \frac{\sigma}{\sigma_0} + 1.74 \cdot \left(\frac{\sigma}{\sigma_0}\right)^{5.42} \tag{36}$$

With the approach from ASTM E646-07 [13], the strain-hardening coefficient n for the air environment experiment, the value is $n = 4.1$, of the same order of magnitude as the one obtained above. Also, it should be noted that the ASTM approach mentioned an error in the results between 5% to 15%.

In Fig. 1 a comparison between the experimental stress-strain curve and those from the equation (36) is displayed for the air environment. To improve the prediction in the elastic domain it was considered also the elastic compliance of the testing facilities.

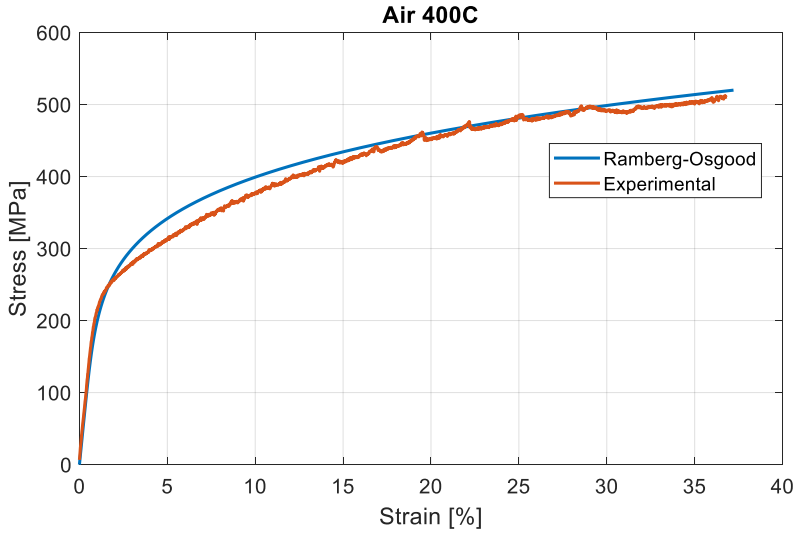

Figure 1. Comparison between experimental and Ramberg - Osgood stress-strain relationships for SSRT in the air at 400°C.

For the evaluation of the errors, Fig. 2 displays the residuals and the standardised residuals.

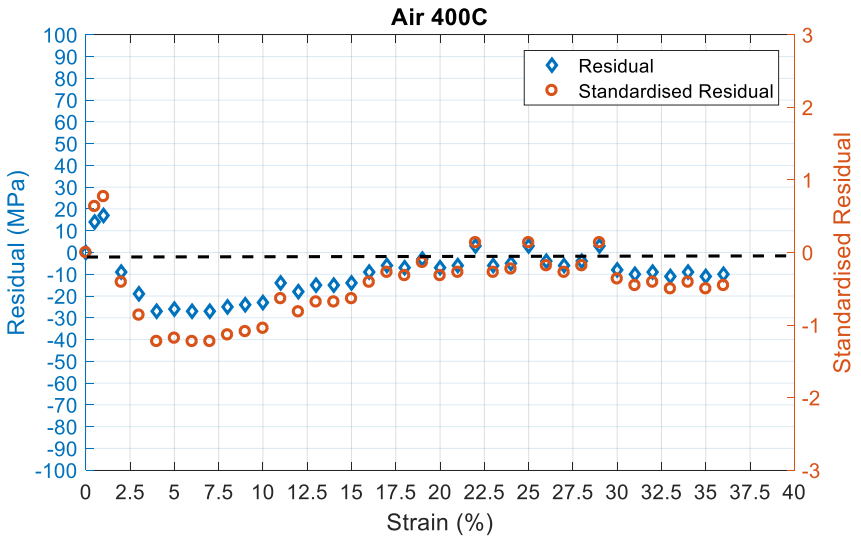

Figure 2. Residuals and the standardised residuals for SSRT in the air at 400°C.

One may see that the Ramberg – Osgood equation gives the predictions in the air environment, in good agreement with the experimental data for the whole domain of strain ($S_{res} < 3$).

In the liquid lead, the Ramberg - Osgood constitutive equation for 316L at 400°C is:

$$\frac{\varepsilon}{\varepsilon_0} = \frac{\sigma}{\sigma_0} + 1.83 \cdot \left(\frac{\sigma}{\sigma_0}\right)^{5.52} \tag{37}$$

With the same approach from ASTM E646-07, the strain-hardening coefficient n for the liquid lead environment experiment, the value is $n = 3.4$, of the same order of magnitude as the one obtained above.

In Fig. 3 a comparison between the experimental stress-strain curve and those from the equation (37) is displayed for the liquid lead environment. Also, the prediction improvement in the elastic domain considered the elastic compliance of the testing facilities.

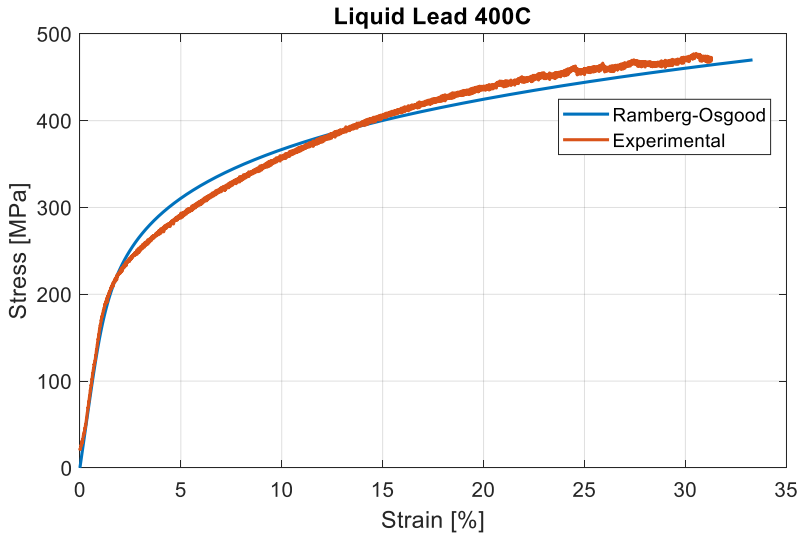

Figure 3. Comparison between experimental and Ramberg Osgood stress-strain relationships for SSRT in the liquid lead at 400°C.

Fig. 4 displays the residuals and the standardised residuals and the Ramberg – Osgood equation gives the predictions in good agreement with the experimental data, in the liquid lead environment, for the corresponding domain of strain ($S_{res} < 3$).

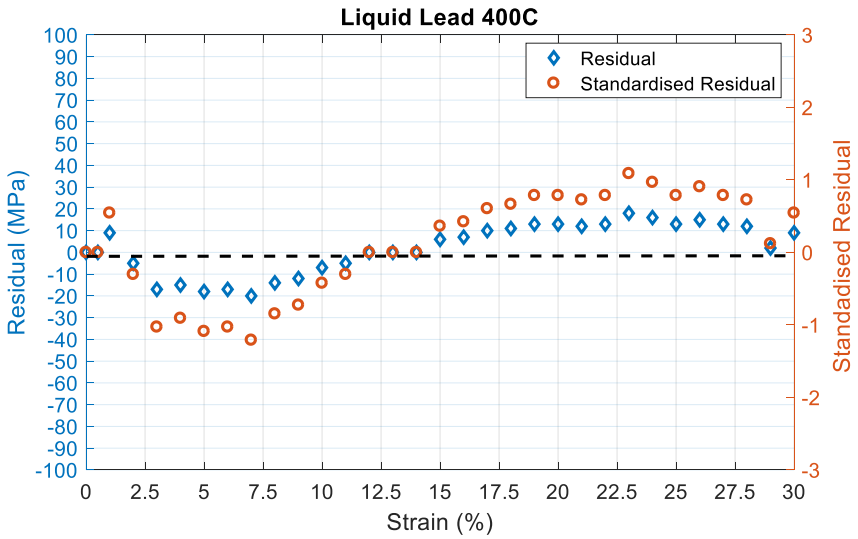

Figure 4. Residuals and the standardised residuals for SSRT in the liquid lead at 400°C.

From the analyses of Figs. 1-4 it can be concluded that the comparisons between the experimental curves and those proposed in relationships (36) and (37) are in good agreement for both test environments (air and liquid lead). In this context, we may note the following features of the method developed here for Ramberg – Osgood parameters:

- The method is easy to be implemented into programming environments (MATLAB) and the numerical solution of the transcendental equation for strain-hardening coefficient is more flexible and faster than solutions existing in other methodologies;
- The parameters α and n obtained with the presented method can describe a whole domain of the experimental curves (elastic and elastic-plastic);
- The accuracy of the prediction was checked with residuals and standardised residuals and the results were quite good.

In the literature, the LME of stainless steel is somewhat distinguished because embrittlement tends to be not so severe compared to most other materials [3]. Hamouche - Hadjem noted some differences for 316L exposed to Pb-Bi in the fracture morphology [21]. From the above analyses two observations result:

- The fracture stress (UTS), decrease around 7-8% in the liquid lead compared to tests in the air;
- The fracture strain decreases around 13-14% in the liquid lead compared to tests in the air.

Even these results could be considered in the scatter range of the experiments, there is a systematic tendency of both parameters. Therefore, we consider that this indicates that the LME is acting on the 316L specimens tested in the liquid lead at 400°C and the phenomenon must be identified in the crack initiation and propagation as well.

5. DESCRIPTION OF THE MODEL FOR SIMULATION OF THE FRACTURE MECHANICS BEHAVIOR UNDER LME CONDITION

To evaluate that the LME influences the mechanical behaviour of the 316L specimens in the liquid lead at 400°C, versus mechanical behaviour in the air, a simulation of the fracture process is conducted by finite element analyses. The analyses of the crack initiation and crack propagation by finite element method uses a model of the Compact-Tension (CT) specimen type, which is recommended by ASTM E1820 [22] in the determination of the fracture toughness material properties and *J*-integral also. The CT model is implemented in the fracture mechanics software, called FEACrack [17], and the model has the specific shape and dimensions as they are mentioned in ASTM E1820 [22], see Fig. 5.

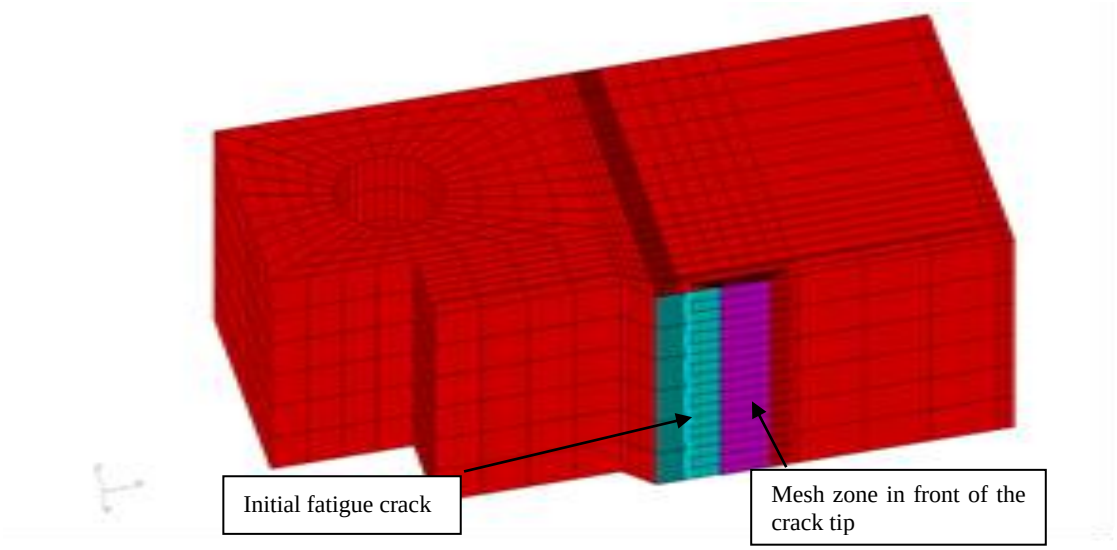

Figure 5. CT model (half) and the finite elements mesh around the crack tip.

The analyses are performed in the elastic-plastic range, therefore to obtain the convergence of stress and strain solutions are needed to implement many steps of the loading. For the loading, it is preferred the displacement control, as is suggested by ASTM E1820.

After some trial analyses performed with FEACrack software, the following specifications for the model are established to be used:

- Program and model options:
  - Analyses type: cell crack mesh for element extinction crack growth;
  - Write results (stresses and strains) at element centroids;
  - Use 8 node brick elements;
  - Use linear kinematic element formulation (small strain).
- Material model type:
  - Use incremental plasticity;
  - Type of plasticity is Ramberg - Osgood model, equation (36) for the air, and equation (37) for the liquid lead;
  - The number of type steps = 150 for a Δz=2mm controlled displacement of the loading pins.
- Gurson - Tvergaard - Needleman model parameters:
  - void interaction parameters: q_1=1.5, q_2=1.0, q_3=2.25;
  - initial porosity: $f_0 = 0.005$;
  - critical porosity: $f_c = 0.15$ for the air and $f_c = 0.10$ the liquid lead;

- mean nucleation strain $\varepsilon_N = 0.3$, with a standard deviation $s_N = 0.1$, and the volume fraction of the nucleating voids $f_N = 0.04$.

To perform crack initiation and propagation, the model takes into account the extinction of finite elements from the crack front. The fact is performed by de-cohesion when the achievement of the critical fraction of voids in the area is reached. The extinction of the finite elements on the front of the advancing crack happens when the material cohesion achieves the critical fraction of voids.

6. RESULTS AND DISCUSSION

From the finite element analyses of the CT model specimen in the air with FEACrack software, Fig. 6 displays the crack front status after 60 steps of loading. Its "tunnelling" shape is typical for the fracture of CT specimen under tensile loading, an aspect that is always revealed in the experimental fracture mechanics tests.

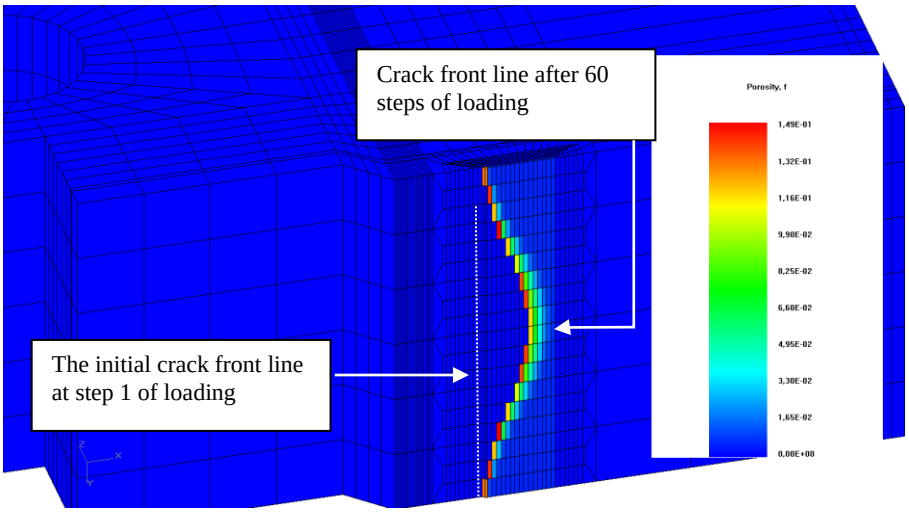

Figure 6. Crack front shape for CT after 60 steps of loading (air).

Same analyses for the CT model specimen in the liquid lead display the crack front status after 60 steps of loading, Fig. 7, and its shape is also typical for the fracture of CT specimen in the experimental tests.

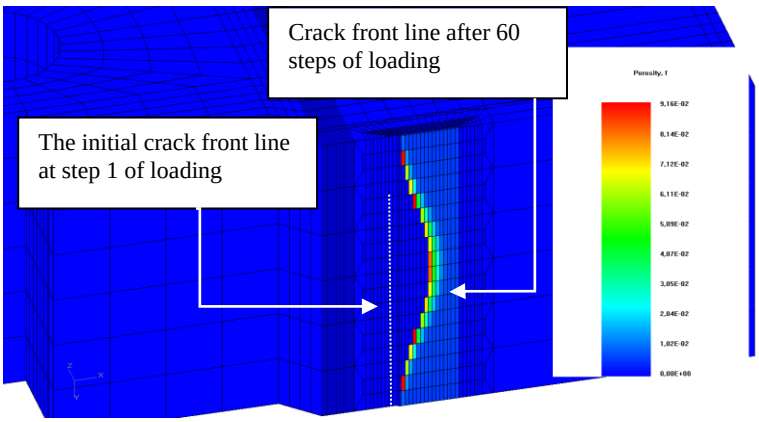

Figure 7. Crack front shape for CT after 60 steps of loading (liquid lead).

A better judgment of the LME response in the liquid lead at 400 °C for the simulation of crack growth model in 316L is revealed in Fig. 8.

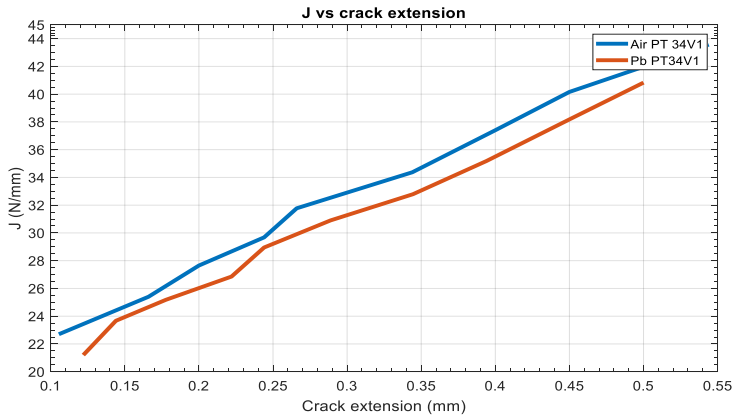

Figure 8. J-integral versus crack extension in the liquid lead compared with air.

Crack extension in the liquid lead is larger than crack extension in the air at the same value of the *J*-integral. This is valid for the whole range of loading, represented here by *J*-integral spectrum values. Two main observations:

- the crack extensions in the liquid lead at the similar *J*-integral values are greater about 10-15%; this is consistent with the decrease of fracture strain in the liquid lead concerning the air obtained in the experimental SSRT tests;
- the corresponding *J*-integral values at the same crack extensions are reduced in the liquid lead concerning the air; this is in line with the results mentioned in reference [1] for the fracture toughness for 316L in the liquid bismuth eutectic (LBE) at 200 °C and 300 °C.

These observations prove that the elaborated model for 316L can simulate fracture mechanics behaviour under LME conditions in the liquid lead at 400 °C and the results are in agreement with the experimental test results and similar mentioned in the literature.

7. CONCLUSIONS

The paper's objective is the development of a model to describe the fracture mechanics behaviour of 316L under liquid metal embrittlement conditions in the liquid lead at 400°C, using the fracture mechanics framework.

The constitutive equations are obtained in the Ramberg - Osgood format and it is proposed a new method to obtain the strain-hardening coefficient from experiments in the air and the liquid lead. The accuracy of the prediction was checked with residuals and standardised residuals and the results were quite good. The method is easy to be implemented into programming environments (MATLAB) and the numerical solution of the transcendental equation for strain hardening coefficient is more flexible and faster than solutions existing in other methodologies. Also, the parameters α and n obtained with the presented method can describe a whole domain of the experimental curves (elastic and elastic-plastic).

The elaborated fracture model uses the finite element analyses of Compact-Tension specimen and it is based on the Gurson - Tvergaard - Needleman approach to perform crack initiation and crack growth. The results put into evidence the LME influence on crack initiation and crack growth for 316L specimens in the liquid lead at 400°C, versus mechanical

behaviour about the air, and they are in good agreement with the experimental test results and similar mentioned in the literature.

The model is practical in the structural integrity activities of the innovative materials that will be used in the ALFRED demonstrator, which will be build-up at RATEN ICN, Romania.

REFERENCES

[1] Nuclear Energy Agency, *Handbook on Lead-bismuth Eutectic Alloy and Lead Properties, Materials Compatibility, Thermal-hydraulics and* Technologies, 2015 Edition, © OECD 2015 NEA No. 7268, 2015.

[2] Kamdar, M.H., *Progress in Materials Science*, **15**, 289, 1973.

[3] Kolman, D.G., *Corrosion*, **75**(1), 42, 2019.

[4] Lucan, D., Valeca, S.C., Jinescu, G., Velciu, L., *Journal of Engineering Sciences and Innovation*, **3**(4), 313, 2018.

[5] Ramberg, W., Osgood, R.W., *Description of stress-strain curves by three parameters. National Advisory Committee of Aeronautics*, Technical Note 902, National Bureau of Standards, Washington D.C., 1943.

[6] Kiran, R., Khandelwal, K., *Gurson model parameters for ductile fracture simulation in ASTM A992 steels*, Wiley Publishing Ltd, Fatigue& Fracture of Engineering Materials & Structures 00, pp. 1-13, 2013.

[7] Gurson, A.L., *Journal Engineering Materials Technology*, **99**, 2, 1977.

[8] Tvergaard, V., Needleman, A., *Acta Metallurgica*, **32**, 157, 1984.

[9] Tvergaard, V., *International Journal of Fracture*, **18**, 237, 1982.

[10] Papirno, R.P., *Computer analysis of stress data: program description and user instructions*, Army Materials and Mechanics Research Center Watertown, Massachusetts 02172, 1976.

[11] Rajendran, R., Venkateshwarlu, M., Petley, V., Verma, S., *Journal Mechanical Behaviour Materials*, **23**(3-4), 101, 2014.

[12] Patwardhan, P.S., Nalavde, R.A., Kujawski, D., *Procedia Structural Integrity*, **17**, 750, 2019.

[13] ASTM E646-07, *Standard Test Method for Tensile Strain-Hardening Exponents (n - Values) of Metallic Sheet Materials*, 2007.

[14] Dieter, G. jr., *Mechanical Metallurgy*, McGRAW-HILL BOOK Company, 1961.

[15] Anderson, T.L., *Fracture Mechanics, Fundamentals and Applications*, CRC Press, 1995.

[16] Matlab R2017b, The MathWorks, Inc.USA.

[17] FEACrack, *3D Finite Element Software for Cracks*, User's Manual, QuestIntegrity, USA.

[18] ASTM G129-00, *Standard Practice for Slow Strain Rate Testing to Evaluate the Susceptibility of Metallic Materials to Environmentally Assisted Cracking*, 2000.

[19] ASTM E8/8M, *Standard Test Methods for Tension Testing of Metallic Materials*, 2016.

[20] Hessling, J.P., *Uncertainty Quantification and Model Calibration Paperback,* InTechOpen, 2017.

[21] Hamouche-Hadjem, Z., Auger, T., Guillot, I., Gorse, D., *Journal of Nuclear Materials*, **376**(3), 317, 2008.

[22] ASTM E1820-11, *Standard Test Method for Measurement of Fracture Toughness*, 2011.